CrossMark

ORIGINAL ARTICLE

Saltwater intrusion in an irrigated agricultural area: combining density-dependent modeling and geophysical methods

N. N. Kourgialas[1] · Z. Dokou[1] · G. P. Karatzas[1] · G. Panagopoulos[2] ·
P. Soupios[3] · A. Vafidis[2] · E. Manoutsoglou[2] · M. Schafmeister[4]

Abstract Saltwater intrusion is one of the most important water quality problems in coastal aquifers, especially in areas with increased water demands. Geophysical techniques can provide a non-invasive and cost-effective approach for determining the geometrical characteristics of an aquifer and for guiding the saltwater intrusion modeling process and in turn reducing the model's inherent uncertainty. In this work, the above concept was applied in the Tympaki basin in Heraklion, Greece. The transient electromagnetic method was used to obtain an accurate 3-D geomodel (bedrock geometry and fault detection) of the basin. This, in turn, was used to guide the construction of a density-dependent groundwater flow and transport simulation model. The results show significant advancement of the saltwater intrusion front in the northern part of the study area, while the phenomenon is less pronounced in the central and southern parts. This is mainly attributed to the combined effect of the fault in the northern part of the basin, the uplifted Neogene deposits in the central part and the freshwater inflow from the Festos corridor in the southern part.

✉ N. N. Kourgialas
nektarios.kourgialas@enveng.tuc.gr

[1] School of Environmental Engineering, Technical University of Crete, 73100 Chania, Greece

[2] School of Mineral Resources Engineering, Technical University of Crete, 73100 Chania, Greece

[3] Department of Environmental and Natural Resources Engineering, Technological Educational Institute of Crete, 73133 Chania, Greece

[4] Institut für Geographie und Geologie, Greifswald University, Greifswald, Germany

Introduction

Saltwater intrusion is one of the major environmental problems in coastal areas due to the serious and irreversible effects on the quality of the water used for drinking and irrigation purposes. The existence of faults in coastal aquifers renders them more vulnerable to saltwater intrusion, because they provide a means for saltwater to enter the aquifer using more rapid flow paths than in homogeneous systems. Thus, the effective prediction tools based on mathematical models that describe the saltwater intrusion phenomenon accurately are of vital importance for the prevention of groundwater contamination in such regions.

Two main approaches have been employed to describe the saltwater intrusion problem in mathematical terms. The simpler of the two approaches is the sharp-interface approach combined with the Ghyben–Herzberg approximation. In this approach, freshwater and seawater are considered as two completely immiscible fluids with different densities that are separated by an interface of a small finite width (Reilly and Goodman 1985). The disadvantage of using the sharp-interface assumption is that it does not take into account the mixing of freshwater and seawater, which is one of the most distinctive features of saltwater intrusion and its dynamics (Abarca et al. 2007). This approach is only valid under steady-state conditions or at early times of transient simulations (Llopis-Albert and Pulido-Velazquez 2014). Various studies have shown that the sharp-interface approximation is conservative in that it overestimates saltwater intrusion and as a result underestimates sustainable pumping rates (Pool and Carrera 2011).

🌀 Springer

The second approach, termed density-dependent flow approach, assumes that the freshwater–saltwater system consists of a miscible fluid transporting a solute that affects the density and viscosity of the fluid. The width of the mixing zone between freshwater and saltwater is significant, as is usually the case in real-world situations, rendering this approach suitable for real-world complex problems. For this reason, the density-dependent approach was adopted in this work.

The application of density-dependent models in real-world applications has recently increased, especially that of 3D models, due to the improvements in speed of computational techniques which enable the use of finer grids and complex model geometries (Abarca et al. 2007). Such field applications have been implemented in coastal aquifers all over the world. For example, in Florida (Panday et al. 1993), in Huangheying, Longkou, China (Xue et al. 1995), in the La Vinuela reservoir system in Malaga, Spain (Garcia-Arostegui et al. 1998), in the Korba coastal plain, Tunisia (Paniconi et al. 2001), in the Netherlands (Essink 2001), in Morocco (Aharnouch and Larabi 2004), in the Kiti aquifer, Southern Cyprus (Milnes and Renard 2004), in Ravena, Italy (Giambastiani et al. 2007), in Santorini, Greece (Kopsiaftis et al. 2009) and in Heraklion, Crete, Greece (Dokou and Karatzas 2012).

The high uncertainty associated with the presence and the dimensions of fractures and faults within a porous medium has tremendous effects on the modeling of subsurface flow and contaminant transport as it results in complex flow path geometry. Cherubini and Pastore (2011) analyzed the effects of geologic structures, such as faults, which can act as conduits or barriers to seawater intrusion. Papadopoulou et al. (2005) performed groundwater flow simulation of a complex karstified aquifer in Crete, characterized by the presence of main faults. The results showed extensive water table depletion along the two main faults. Papadopoulou et al. (2010) also simulated a complex karstified aquifer system with the presence of main faults and they concluded that they drastically affect regional flow. Dokou and Karatzas (2012) investigated the effect of fractures on saltwater intrusion in a karstified coastal system using both density-dependent modeling and the sharp-interface approach. They concluded that the sharp interface overestimates the saltwater intrusion in many cases and that the combination of equivalent porous media and the discrete fracture approach can accurately represent the fractured aquifer system.

The fundamental problem that modelers face when trying to simulate a heterogeneous physical system is the lack of information regarding the system's parameters, hydraulic characteristics and their distribution. Geophysical studies can fill that gap by providing information regarding the location and characteristics of fractures and faults.

The main objective of this study is the development of a saltwater intrusion prediction tool for the prevention of water pollution in agricultural coastal regions. The contribution of this study is to introduce an integrated approach for monitoring and modeling saltwater intrusion by combining geophysical methods and a density-dependent simulation model for fractured media. The key idea in this approach is to develop a comprehensive geophysical data processing tool which guides the modeling process and provides additional hydrogeological parameter information. First, a detailed geological mapping of the study area is carried out prior to any other survey. Several electromagnetic geophysical measurements are collected next by applying the TEM method. Finally, a three-dimensional, density-dependent groundwater flow and transport model that takes into consideration all the geomorphologic characteristics, hydrogeological and geophysical data of the aquifer system is constructed. This methodology was applied to the coastal aquifer system of Tympaki in Crete, Greece.

Study area

The Tympaki clastic aquifer is characterized by alluvial sediments that fill the 50 km^2 coastal Tympaki basin since Mio-Pliocene. Marly deposits of middle to late Miocene are considered as the practically impermeable bottom of the aquifer. As a result of an intensive tectonic history, the basin exhibits segmentation into several fault-bounding blocks. These blocks have undergone differential vertical movements which resulted in differences in the thickness of the aquifer (Panagopoulos et al. 2013). Morphologically, the basin is differentiated into a coastal plain to the west and a hilly area to the east.

The Tympaki basin is located in the southwestern part of the Heraklion Prefecture in central Crete and represents a westwards tectonic extension of the larger alluvial plain of the Messara basin (Fig. 1a). Specifically, sedimentation in the Messara basin started during the Middle Miocene and resulted in the deposition of sequences of fluvio-lacustrine and alluvial deposits, conglomerates, cobbles, sands, marls and clays with abrupt lateral and vertical lithological changes. According to the results from previous studies (FAO 1972; Paritsis 2005; Vafidis et al. 2014a, b; Soupios et al. 2014), the borders of the basin are the tectonic contact of the permeable deposits with the practically impermeable Neogene formations. The existence of three additional normal faults (from NNW to SSE) that configure crucially the geometry of the Tympaki basin was suggested by the results of the MEDIS program (FAO 1972; Paritsis 2005) as shown in Fig. 1b. A generalized geological cross section representing the conceptual model of the area is presented
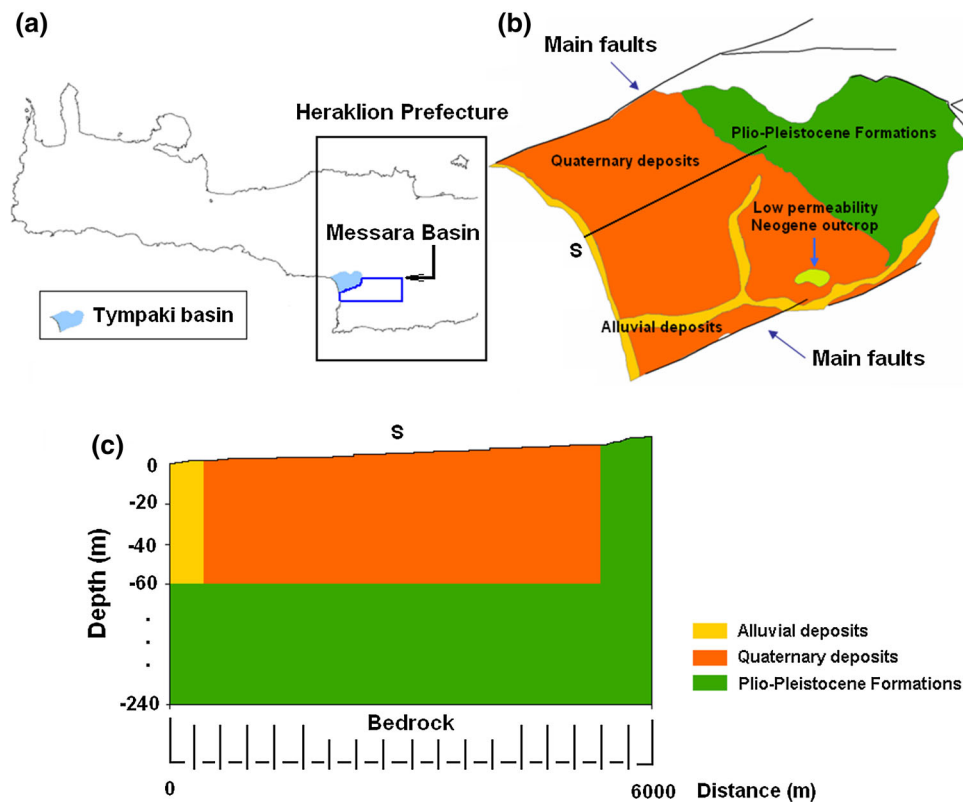
Fig. 1 **a** The broader study area showing the Tympaki and Messara Basins and the Heraklion Prefecture in Crete, Greece (**b**) original geological information and location of cross-section S, (**c**) conceptual geological cross-section S, showing the vertical geological distribution

in Fig. 1c. Moreover, the elevation of the Tympaki basin ranges from zero to 460 m a.m.s.l.

The average annual aquifer recharge from rainfall infiltration and irrigation return amounts to 11 Mm^3. Moreover, 0.5 Mm^3 flows into the aquifer from the neighboring Messara basin whereas 1.2 Mm^3 of seawater enters on average, the aquifer every year along its coastal front. Discharge to the sea, of mostly fresh water with a relative small proportion of saline water, amounts, on average, to 7 Mm^3 per year. Rainfall in the area is low (less than 500 mm per year) and according to Paritsis (2005), the aridity classification of the study area is close to semi-arid conditions. Despite these unfavorable climatic conditions, intense agricultural activity occurs.

The rapid economic development in the last 30 years has exerted strong pressures on many sectors in the region. The agricultural and touristic growth in the Tympaki basin has strong impact on the water resources and the ecosystem of the area due to the substantially increasing water demand. The economy of the region is based on agriculture with intensive cultivation, mainly of olive trees, grapes, citrus and vegetables in green houses and touristic activities consuming large amounts of drinking water. According to previous studies, a dramatic drop of more than 30 m in the mean groundwater level was recorded in the last years

(1989–2002). The depletion of the aquifer has reduced water availability, as groundwater is the only resource for irrigation. The causes can be traced to uncontrolled pumping as more than 4000 hectares of olive groves and greenhouse vegetables are irrigated by mainly groundwater extraction amounting to 14,315,000 m^3 per year. The population of the Tympaki municipality is approximately 10,000 and the drinking water needs are close to 1,180,000 m^3 per year. The uncontrolled pumping has led, in turn, to serious saltwater intrusion in the coastal area of the Tympaki basin (Paritsis 2005). The saltwater intrusion phenomenon in the area has been observed in the past 40–50 years and is more intense close to the coast. No evidence exists that supports the occurrence of connate water, thus the sea is assumed to be the only source of salinization of the freshwater reserves of the aquifer.

Methodology

Geophysical methods (TEM and 3-D modeling)

The TEM method has been used in hydrogeological studies over the last decades. Detailed information about the method can be found in several textbooks and research

articles (Kaufman and Keller 1983; Fitterman and Stewart 1986; Stewart and Gay 1986; Goldman et al. 1988; Mills et al. 1988; Nabighian and Macnae 1991; McNeill 1994; Sharma 1997; Kanta et al. 2013; Reynolds 2010).

TEM belongs to the class of controlled source electromagnetic methods. The acquisition system consists of a transmitter (Tx) loop and a receiver (Rx) loop of varying sizes depending on the exploration depth. A current flowing through the Tx loop generates a primary, stationary field. Using an abrupt on–off switching sequence, currents are induced into the ground according to Faraday's law. The current will decay and further induce a secondary magnetic field which is measured in the Rx loop. The decay rate of the electromagnetic field depends on the distribution of the resistivity in the subsurface. Based on this principle, the voltage measured on the Rx coil can provide information about geoelectrical structures (Barsukov et al. 2006).

The penetration/exploration depth is controlled by the time interval between subsequent turn-off and next turn-on. As the time interval increases, the current intensity migrates to greater depths and the measured secondary field will depend more on the properties of deeper layers. Contrary to other geophysical methods, the TEM method can eliminate the near-surface resistivity variation providing high-quality data (Barsukov et al. 2006; Soupios et al. 2010).

The TEM survey was carried out using a single square loop configuration (used as transmitter and receiver) with dimensions 50 m × 50 m, allowing an interpretation of the data of the subsurface resistivity structure for a maximum depth of 100–120 m. In total, 367 soundings were collected at 107 locations (April 2013). The calculated root mean square (RMS) error of the final data set was less than 3.5 %. The raw data were tested, edited or removed depending on their significance. The data were transformed from apparent resistivity with time $[\rho_\alpha(t)]$ to resistivity change with depth $[\rho(h)]$ or the data were inverted using an initial model and defining the appropriate inversion parameters into the inversion algorithm (Barsukov et al. 2006).

For 3-D modeling, an algorithm originally presented by Druskin and Knizhnerman (1988) was applied. Only early times, $t = 8$–250 microseconds, from the TEM responses (curves) and with error of measurements less than 10 % were used to increase the accuracy of the final 3-D model. The raw data were also processed by applying 3-D inversion. Topographic corrections were also applied for processing.

Density-dependent transport model

The finite element density-dependent subsurface flow and transport simulation system FEFLOW were used for modeling the coastal aquifer of Tympaki. According to the density-dependent approach, freshwater and seawater are considered as two miscible fluids with a mixing zone of significant width in-between. The main assumptions of this approach are: (1) the porous medium is considered rigid and saturated, (2) the incompressibility condition, namely the Boussinesq approximation, holds, (3) fluid viscosity depends on concentration, (4) fluid motion can be adequately described by Darcy's law, and (5) dispersion is a property of the porous medium alone that follows the Fickian dispersion law. Under these assumptions, the saltwater intrusion phenomenon can be described by the governing density-dependent flow and mass transport equations and Darcy's law. A detailed description of the density-dependent flow and transport equations appears in Diersch (1988).

The hydraulic head at each location depends on the saltwater concentration. Since the model requires freshwater hydraulic heads as input, an equivalent hydraulic head needs to be calculated when applying boundary conditions and when comparing model results to field data. The required transformation is performed using an equation that relates hydraulic heads to depth, under the assumption that saltwater density varies linearly with depth:

$$h_f = (1 + \alpha)h - \alpha z,$$

$$\alpha = \frac{\rho_s - \rho_f}{\rho_f},$$

where h_f is the equivalent freshwater head; h is the measured head; α is the density difference ratio; ρ_s is the saltwater density; ρ_f is the freshwater density; and z is the elevation.

To calculate the density difference ratio for the field data, the density of the freshwater–saltwater mixture at each well is required. If a chloride concentration measurement is available for a well, then this measurement is used to calculate the density difference ratio and the equivalent freshwater head at the particular well. If the well chloride concentration is unknown, measurements from adjacent wells can be used instead (Dokou and Karatzas 2012).

An important concern when modeling saltwater intrusion is how to accurately represent the dynamic process of inflow-outflow concentrations at the sea boundary. Water entering the domain should have a freshwater concentration while water exiting the domain has an unknown concentration. The model must be able to calculate this unknown concentration. This is handled using a boundary condition of constant concentration $C = C^R$ at the coastal boundary while at the same time imposing a constraint of zero mass flux $Q_C^{\min} = 0$ on the same boundary (Diersch

and Kolditz 2002). This constraint results in a decrease in salt concentration in the upper parts of the aquifer due to the zero dispersive flux along the out-flowing part of the sea boundary (Kopsiaftis et al. 2009).

Regarding the modeling of fractures, a combination of a three-dimensional equivalent porous medium with discrete features was applied. This approach provides flexibility in modeling complex systems (Diersch 2002) such as the coastal aquifer considered in this work. The equivalent porous medium is used to represent the matrix structure of the aquifer system and the discrete features for the simulation of channels, rivers or wells (one-dimensional features), runoff processes and fractures or faults (two-dimensional features). In this work, the main fractures and faults encountered at the field site are represented by two-dimensional discrete feature elements that follow the Hagen–Poiseuille law:

$$v = -Kf_\mu(\nabla h + \alpha\eta_j)$$

$$K = \frac{b^2\rho_f g}{12\mu_f}I$$

where v is the fluid velocity, f_μ is a viscosity constitutive relationship; h is the freshwater hydraulic head; η_j is the gravitational unit vector; b is the fracture aperture; μ_f is the viscosity; and I is the unit (identity) tensor.

Groundwater flow and transport model development

The horizontal discretization of the unconfined aquifer was implemented using a triangular finite element mesh consisting of 4010 nodes and 7670 elements. The vertical discretization of the model area was based on boring log information provided by Panagopoulos et al. (2013). The conceptual model comprises a 240 m deep unconfined aquifer, discretized in 12 numerical layers (13 Slices). The elevation of the model's top layer is variable following the relief (DEM of 10 m × 10 m) and the rest of the layers have a thickness of 20 m.

The hydraulic conductivity was set to 25 m/day for the neogene formations, 180 m/day for the Plio-Quaternary deposits, 200 m/day for the alluvial deposits and 1 m/day for the small low permeability lens encountered in the southern part of the basin. These values were based on hydraulic conductivity estimates from previous studies in the area (Paritsis 2005). The porosity was estimated at 0.3 and the longitudinal and transverse dispersivities were obtained from model calibration at 45 and 4.5 m, respectively.

The model was run in transient mode for a period of 32 years (April 1982–April 2014) divided in two seasons (wet and dry), accounting for seasonal variations in rainfall, pumping activities, infiltration and lateral influx rates. An automatic time step control was used to overcome numerical difficulties in solving the non-linear equations.

Flow boundary conditions

The equivalent hydraulic head was calculated by applying boundary conditions and comparing model results to field data. A first type flow boundary condition was set along the coastline (zone 1 in Fig. 2). For the first layer, the hydraulic head was set to zero and for the rest of the layers it was set to the equivalent freshwater head, assuming a saltwater density of 1025 kg/m^3. Pumping wells were

Fig. 2 Mesh density, boundary conditions (zones 1–5) and observation wells (1–13) for flow or/and mass concentration monitoring
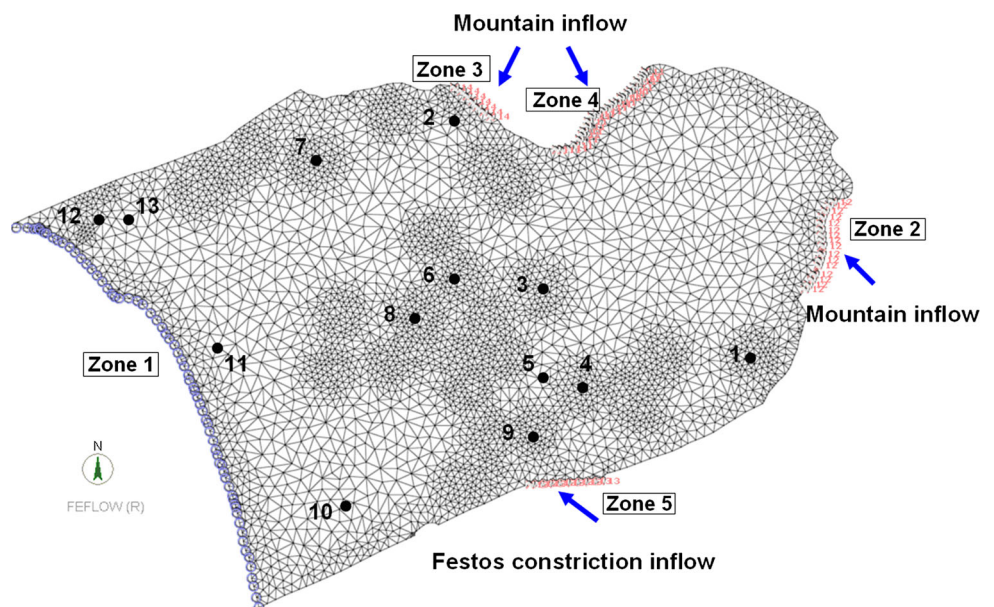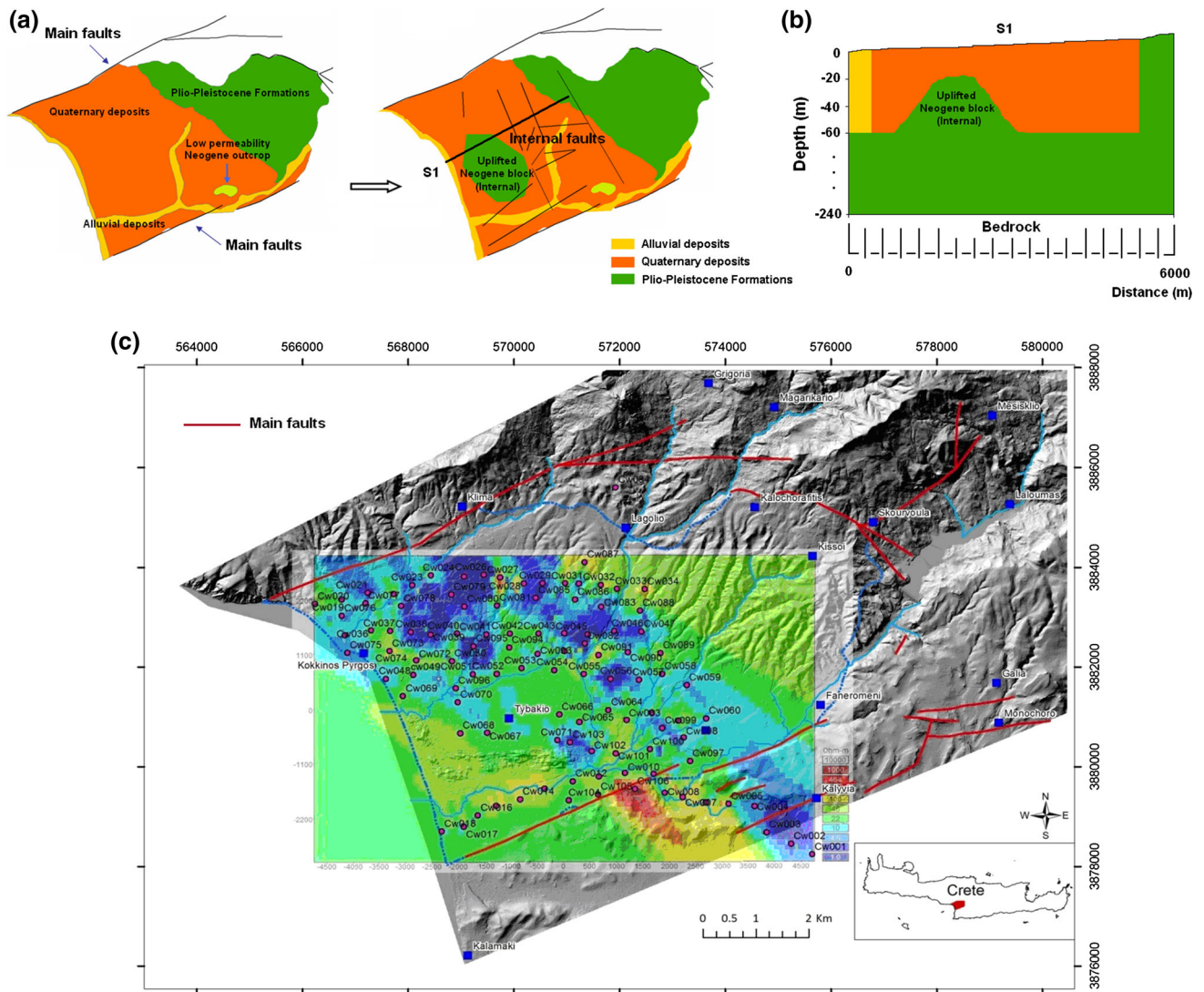
Fig. 3 **a** Original and updated geological information based on the 2-D interpretation of the geoelectrical models, (**b**) updated conceptual geological cross-section S1, (**c**) a slice at depth 50 m below ground surface (*red* and *blue colors* represent the resistive and conductive layers, respectively)
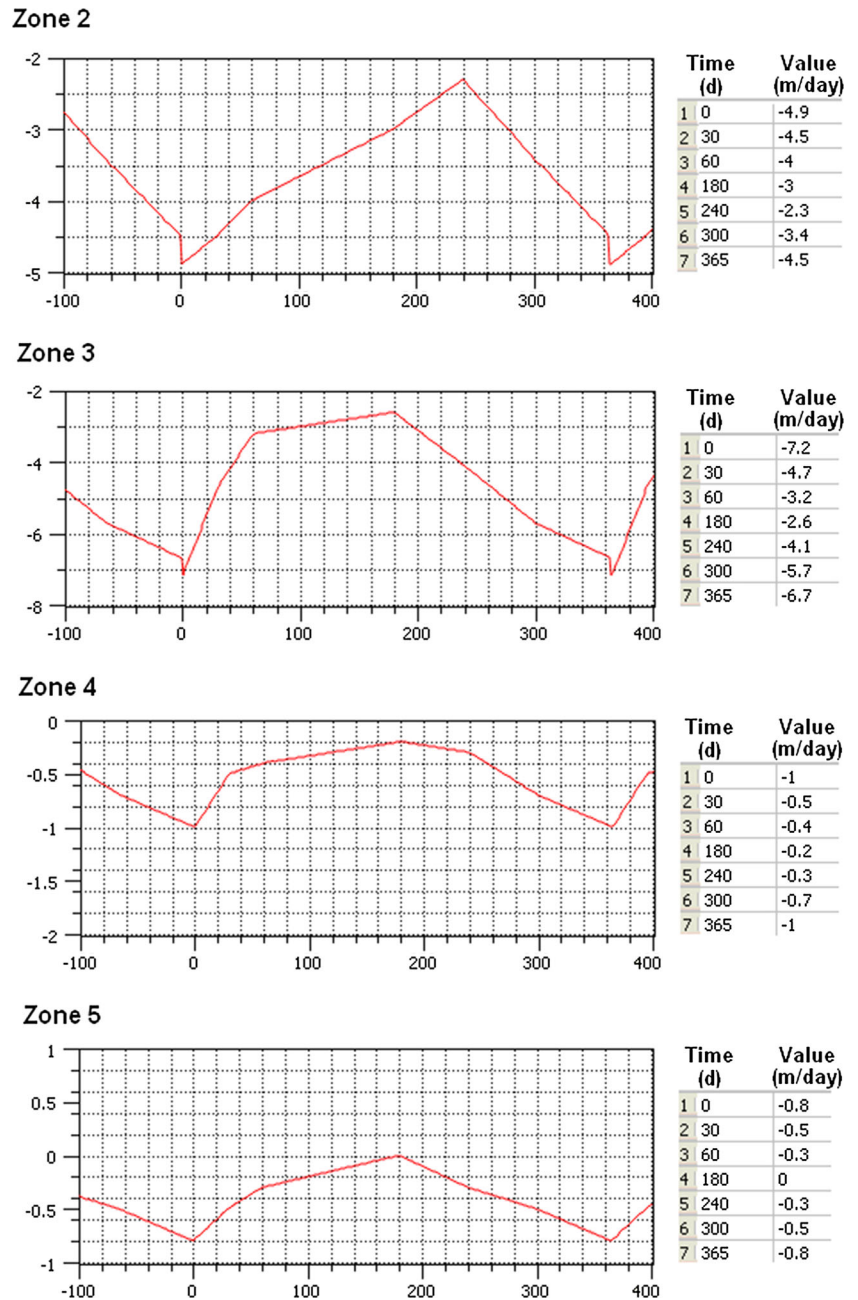
defined as second type boundary conditions and their screens were set at the third layer (alluvial deposits). According to previous studies, the main influx in the Tympaki basin is from the Festos corridor, where a second type boundary condition was set (Festos constriction inflow). The above information was obtained by a hydrogeological report conducted in the area (Paritsis 2005). A smaller inflow originating from the mountainous area was also included in the model during the calibration process (Fig. 2). An average monthly infiltration rate (as 30 % of measured precipitation) was included as an inflow parameter on the top layer of the model assuming no spatial variability due to the small size of the basin. The minimum

and maximum values of infiltration for the summer and winter months were $0–1.6 \times 10^{-4}$ and 4.25×10^{-4}–1.06×10^{-3} m/day, respectively.

Mass transport boundary conditions

A first type mass boundary condition was imposed along the coastline with a constant value of 19,000 mg/l of chloride concentration. This value is based on field measurements of saltwater taken directly from the sea in the northern part of the Heraklion Prefecture. This boundary condition was coupled with an additional constraint as discussed in the previous section.

Fig. 4 Calibrated flow rate time series for zones 2–5 (boundary conditions)

Zone 2

	Time (d)	Value (m/day)
1	0	-4.9
2	30	-4.5
3	60	-4
4	180	-3
5	240	-2.3
6	300	-3.4
7	365	-4.5

Zone 3

	Time (d)	Value (m/day)
1	0	-7.2
2	30	-4.7
3	60	-3.2
4	180	-2.6
5	240	-4.1
6	300	-5.7
7	365	-6.7

Zone 4

	Time (d)	Value (m/day)
1	0	-1
2	30	-0.5
3	60	-0.4
4	180	-0.2
5	240	-0.3
6	300	-0.7
7	365	-1

Zone 5

	Time (d)	Value (m/day)
1	0	-0.8
2	30	-0.5
3	60	-0.3
4	180	0
5	240	-0.3
6	300	-0.5
7	365	-0.8

Results and discussion

Geophysical survey results and contribution to the FEFLOW model setup

The processed TEM soundings (1-D models) were combined by interpolation to produce 2-D pseudo-sections in different directions depending on the expected tectonic discontinuities (faults). These resistivity sections were used to confirm possible (buried) faults or to depict new ones. Apart from the main faults striking in an NW–SE direction, some small internal faults were detected in the NW–SE and NE–SW directions (Fig. 3a) using the geophysical measurements collected in this study and following the results of the lithostratigraphic model of the basin (Panagopoulos et al. 2013). Based on the above findings, the original geological map was updated to include the newly detected small internal faults and is shown in Fig. 3a. In the FEFLOW modeling, the aperture of these faults was considered to be 2 m, while the aperture for the main faults suggested by previous studies (FAO 1972; Paritsis 2005) was estimated at 5 m. A generalized geological cross section (S1) containing the uplifted neogene block representing the updated

conceptual model of the area used in the FEFLOW modeling is presented in Fig. 3b.

Several depth slices were constructed from the calculated 3-D resistivity model. The resistivity slice at depth 50 m below ground surface is presented in Fig. 3c. The depth slice shows mainly faults striking in an NW–SE direction and a low resistivity zone in the northern part of the study area along one of these faults. These conductive zones may be attributed to saltwater intrusion. The results were further compared with borehole logs in the area (Panagopoulos et al. 2013) and were used as input for groundwater flow modeling.

In addition, an uplifted low conductivity block of Neogene marly deposits was detected near the coastline which could play a catalytic role in obstructing the saltwater invasion towards the mainland, affecting the final shape of the saltwater intrusion front (Fig. 3a).

All the above newly available information was applied to the numerical FEFLOW model resulting in an improved assessment tool for predicting saltwater intrusion in the area as compared to the previous modeling approach of Paritsis (2005). In addition, the numerical model presented here was run for the period of April 1982–April 2014, while the Paritsis (2005) model (SEAWAT) was run for the period of October 1968–September 1987.

FEFLOW model

The model was calibrated in two stages. Firstly, the flow model was calibrated by matching the hydraulic heads derived by the FEFLOW model to the observed groundwater levels at eleven different wells (1–11) located in the study area (Fig. 2) for April 2002. The lateral influx rates were used as a calibration parameter for the flow model. The second stage of the calibration process concerns the mass transport model that was calibrated using available chloride concentrations for a limited number of wells (9–12) and three different time periods. Specifically, chloride concentration measurements collected in 1995, 2002, and 2014 for wells (9–12) were used for the mass calibration process. The longitudinal and transverse dispersivities were considered as calibration parameters for the mass transport model.

Due to the seasonal variability of groundwater inflow in the study area, the appropriate time series boundary conditions were determined through the process of calibration, using the trial and error method. Specifically, fixed and time-varying boundary conditions were identified for five parts of the study area. Zones 2, 3, 4, and 5 were defined as time-varying flow boundary conditions of second type (flux). The time-varying groundwater boundary condition for zones 2–5 is presented in Fig. 4. The obtained simulation results show a very small deviation in comparison with the corresponding real-time measurements at the eleven boreholes, since the value of the RMSE is 2.08 m (Fig. 5). Figure 6 shows the 2-D representation of the hydraulic heads and hydraulic head contours in Slice 3.

Regarding the mass transport calibration process, the very good correlation between field measurements and simulation results is shown in Fig. 7. This good fit between observed data and simulation output (RMSE = 52.75 mg/l) was obtained for the flow calibration. Moreover, Fig. 8 shows the 2-D representation of the mass transport results
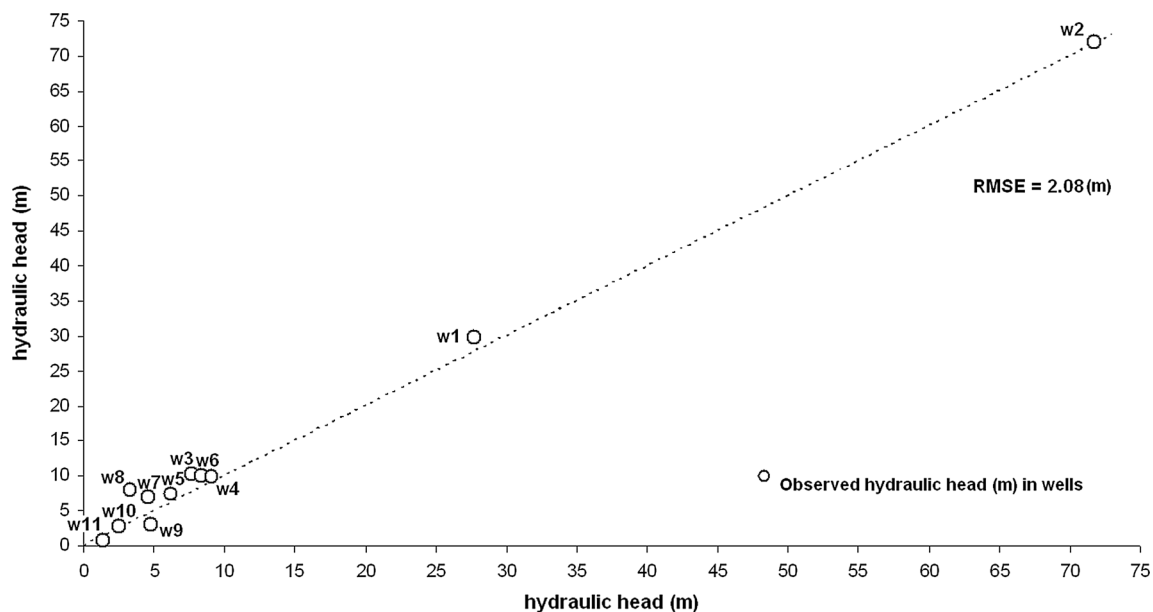

Fig. 5 Comparison of observed (*open circles*) and calculated (*dotted line*) hydraulic head values
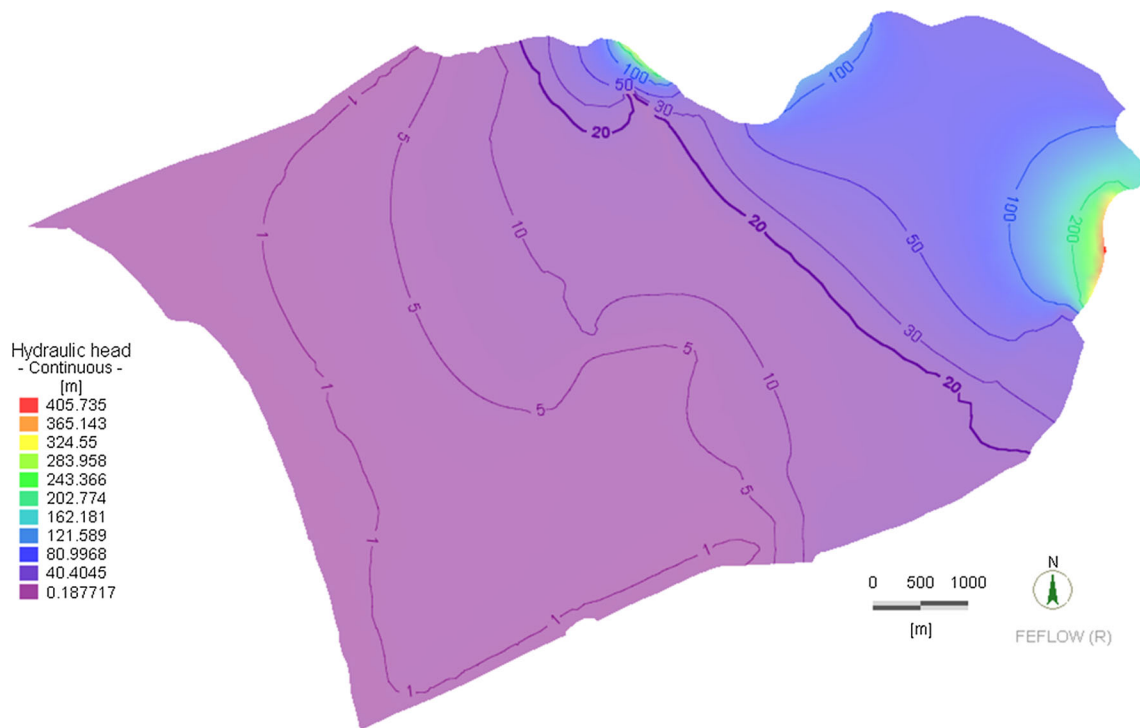
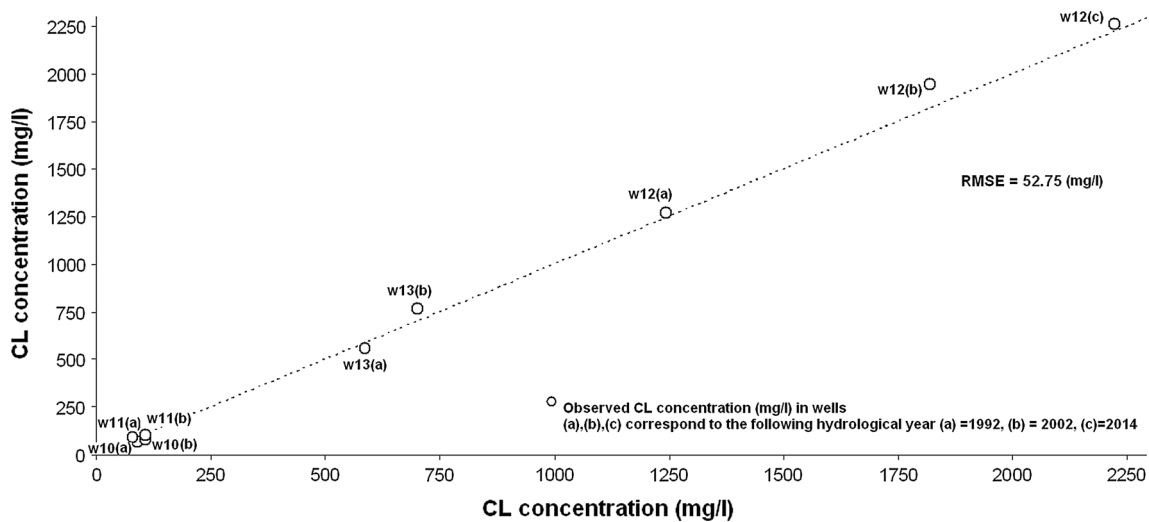**Fig. 6** Flow model results (hydraulic head contours in m), Slice 3

Fig. 7 Comparison of observed (*open circles*) and calculated (*dotted line*) chloride concentration (years: 1992, 2002, and 2014)

for chloride concentrations (mg/l) and the mass concentration isoline of the maximum permitted level of 250 mg/l in Slice 3, for years 1995 and 2014. As observed, the NW–SE faults serve as a means of rapid transport of saltwater contamination to the mainland and in combination with the lower permeability lens (Neogene) located in the central part of the basin they drive the seawater intrusion front asymmetrically inland. The results from the numerical model show intensive saltwater intrusion through the main faults of the study area, while in the central part the phenomenon is less pronounced due to the Neogene deposits that have been raised as suggested by the 3-D geophysical model. Additionally, Fig. 8 shows that the saltwater intrusion zone has extended significantly from 1995 to 2014, when the exploitation of the aquifer was dramatically increased due to the intensive irrigation needs, and reaches up to 700 m especially in the northwestern part of the study area.
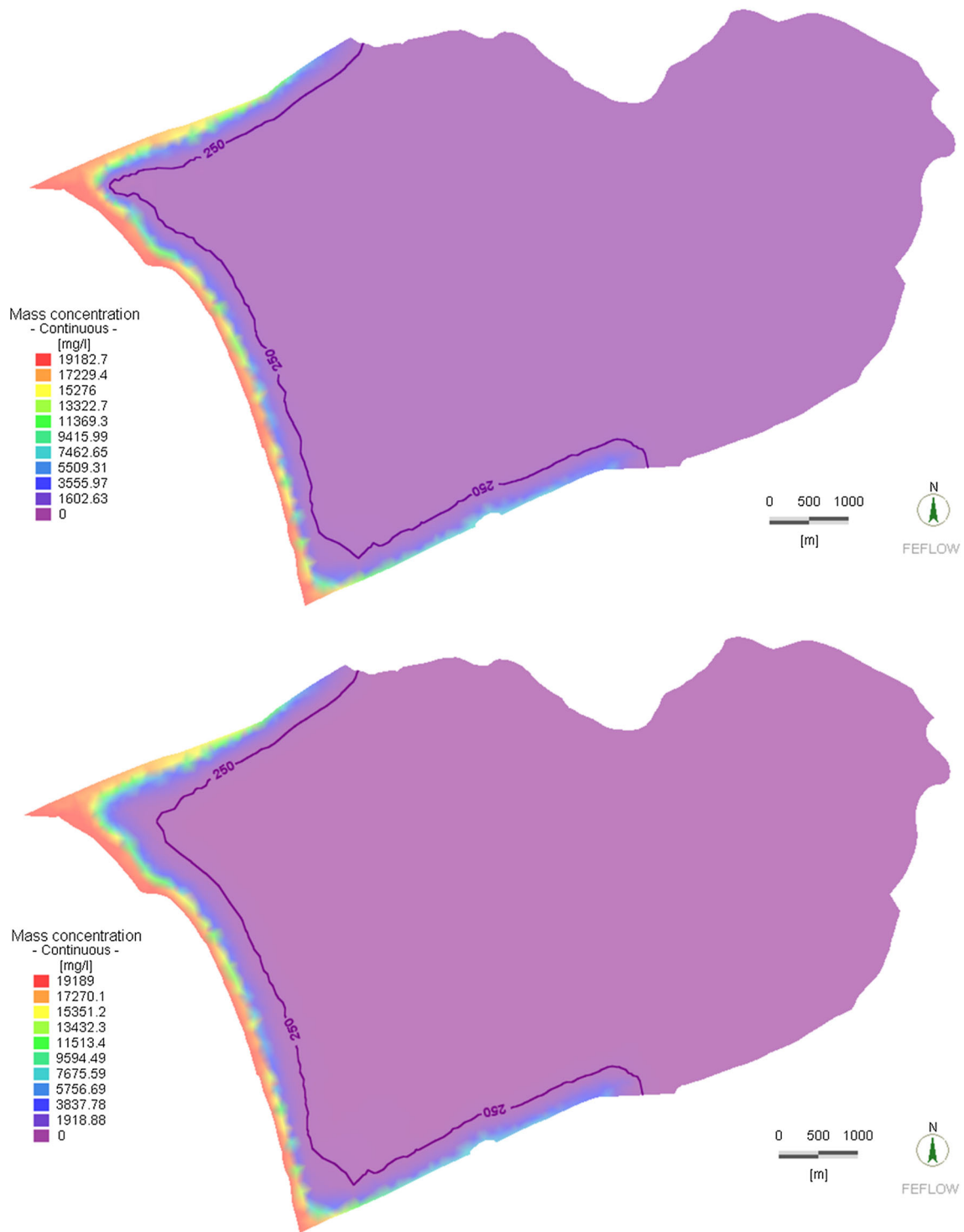
Fig. 8 Mass transport results for chloride concentrations (mg/l) and mass concentration isoline of the maximum permitted level of 250 mg/l for years 1992 (*top figure*) and 2014 (*bottom figure*), Slice 3

Figure 9 shows the chloride concentration along three representative cross sections (mass lines 1, 2 and 3). The saltwater intrusion front has advanced almost 200 m along the southern part (mass line 1), about 400–500 m along the central part (mass line 2) and about 700–800 m along the southern part of the coast (mass line 3). According to the model developed here, which was based on the new information obtained from the geophysical studies, this
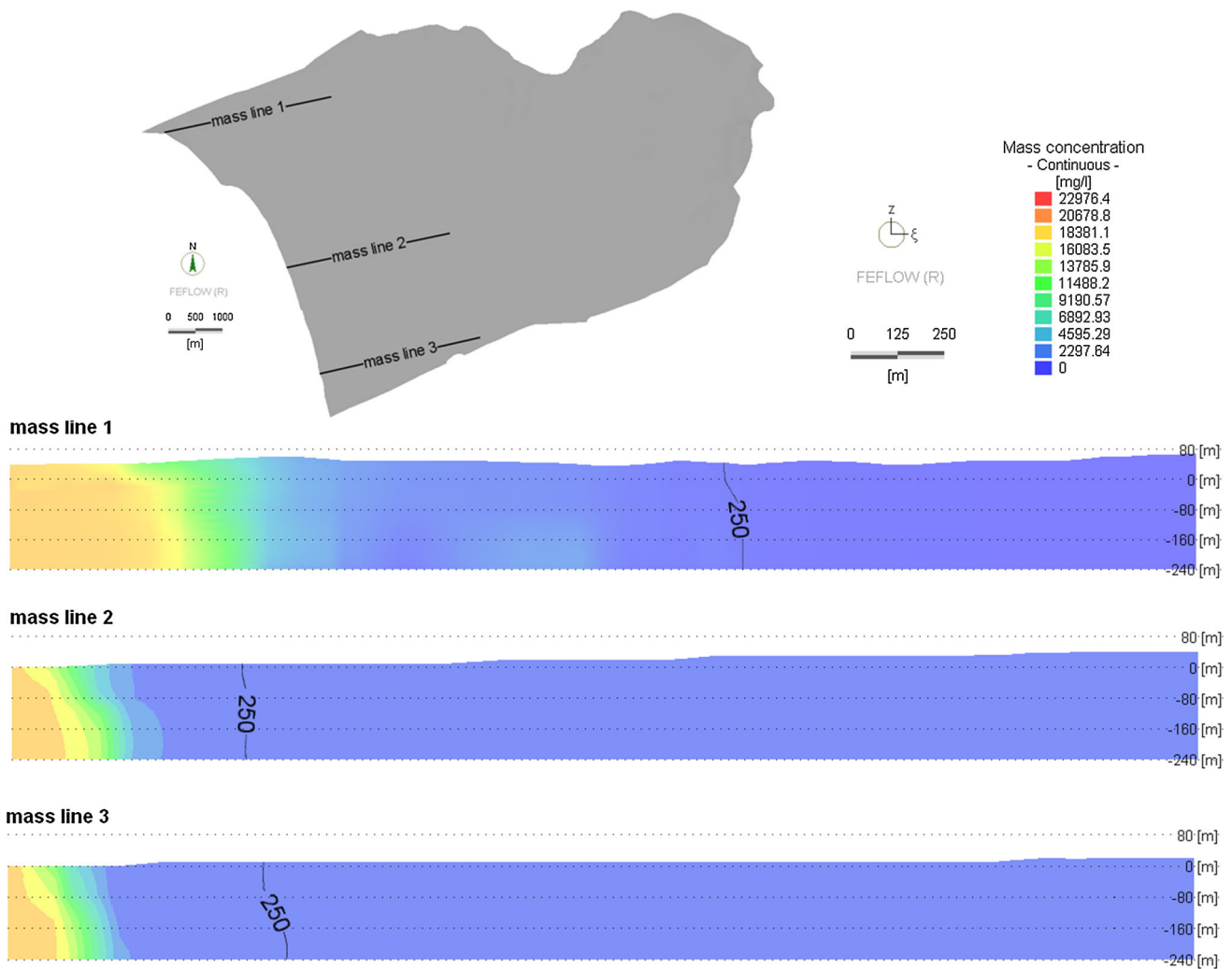
Fig. 9 Chloride concentration along three representative cross sections (mass lines 1, 2 and 3)

variation between the northern, central and southern parts of the coast is attributed to the newly found existence of the uplifted neogene deposits in the center of the basin that hinders the advancement of the saltwater intrusion front and addition to the freshwater inflow from the Festos corridor to the south.

The above results are consistent with previous studies that have modeled the saltwater intrusion phenomenon in the area of Tympaki (Paritsis 2005). Paritsis (2005) used the variable density model SEAWAT and simulated the phenomenon from October 1968 to September 1987. The results of this study show that the saltwater intrusion front lies about 1500 m from the coastline at the northern end of the coast, while at the southern end it lies at about 500–600 m from the coastline. It is evident that during the 27 years that have passed the saltwater intrusion front has advanced rapidly on the northern part and slowly on the southern part of the basin due to the fault and freshwater inflows in these regions, respectively.

Conclusions

The integrated study presented here emphasizes that the combined use of geophysical techniques and groundwater flow and transport modeling can provide a useful tool for monitoring, modeling and managing saltwater intrusion. This tool can prove extremely useful when studying complex hydrogeological areas, such as the Mediterranean costal aquifer of Tympaki in Crete, Greece. In this area, the saltwater intrusion problem has intensified in the last decades due to the increased water demand for irrigation and drinking purposes, especially in the summer months. The results from the density-dependent numerical model, which has been enhanced by the geophysical data, show significant advancement of the saltwater intrusion front in the northern part of the study area, while in the central and southern parts the phenomenon is less pronounced. This is mainly attributed to the combined effect of the northern fault originating from the coast, the uplifted Neogene

deposits in the central part of the basin as suggested by the 3-D lithostratigraphic model, and the freshwater inflow from the Festos corridor to the south.

To provide sustainable growth and maintain the future quality of water resources in the area, a combination of management options such as reduction of pumping activity, artificial recharge and/or collection of precipitation in small scale hydraulic structures such as tanks, could be considered.

Highlights

- Development of a saltwater intrusion prediction tool for complex hydro-geological areas.
- Combination of a 3D density-dependent modeling approach with geophysical techniques.
- Use of discrete features methodology for representing faults in the numerical model.

References

Abarca E, Carrera J, Sanchez-Vila X, Voss CI (2007) Quasi-horizontal circulation cells in 3D seawater intrusion. J Hydrol 339(3–4):118–129

Aharnouch A, Larabi A (2004) A 3D finite element model for seawater intrusion in coastal aquifers. Dev Water Sci 55:1655–1667

Barsukov PO, Fainberg EB, Khabensky EO (2006) Shallow investigation by TEM-FAST technique: methodology and case histories. In: Spichak VV (ed) Methods of geochemistry and geophysics, vol 40. Elsevier, Amsterdam, pp 55–77

Cherubini C, Pastore N (2011) Critical stress scenarios for a coastal aquifer in southeastern Italy. Nat Hazards Earth Syst Sci 11:1381–1393. doi:10.5194/nhess-11-1381-2011

Diersch HJ (1988) Finite-element modeling of recirculating density-driven saltwater intrusion processes in groundwater. Adv Water Resour 11(1):25–43

Diersch HJG (2002) Discrete feature modeling of flow, mass and heat transport processes by using FEFLOW. WASY, Berling

Diersch HJG, Kolditz O (2002) Variable-density flow and transport in porous media: approaches and challenges. Adv Water Resour 25(8–12):899–944

Dokou Z, Karatzas GP (2012) Saltwater intrusion estimation in a karstified coastal system using density-dependent modelling and comparison with the sharp-interface approach. Hydrol Sci J 57(5):985–999

Druskin VL, Knizhnerman LA (1988) Spectral differential-difference method for numerical solution of three-dimensional nonstationary problems of electric prospecting. Izvestiya' Earth Phys 24(8):641–648 (UDC 550.837.3)

Essink GHPO (2001) Salt water intrusion in a three-dimensional groundwater system in the Netherlands: a numerical study. Transp Porous Med 43(1):137–158

FAO (1972) Study of the water resources and their exploitation for irrigation in eastern Crete—Greece. Drillings and pumping tests in Messara AGL:SF/GRE 17/31 tech. rep. 26, UNDP, Iraklio

Fitterman DV, Stewart MT (1986) Transient electromagnetic sounding for groundwater. Geophysics 51:995–1005

Garcia-Arostegui JL, Padillia F, Cruz-Sanjulian JJ (1998) Numerical simulation of the influence of the La Vifluela reservoir system on the coastal aquifer of the Velez River. Hydrol Sci J 43(3):459–477

Giambastiani BMS, Antonellini M, Essink GHPO, Stuurman RJ (2007) Saltwater intrusion in the unconfined coastal aquifer of Ravenna (Italy): a numerical model. J Hydrol 340(1–2):91–104

Goldman M, Arad A, Kafri U, Gilad D, Melloul A (1988) Detection of freshwater/seawater interface by the time domain electromagnetic (TDEM) method in Israel. Naturwet Tijdsehr 70:339–344

Kanta A, Soupios P, Barsukov P, Kouli M, Vallianatos F (2013) Aquifer characterization using shallow geophysics in the Keritis Basin of Western Crete, Greece. Environ Earth Sci 70(5):2153–2165. doi:10.1007/s12665-013-2503-z

Kaufman A, Keller G (1983) Frequency and transient soundings. Methods in geochemistry and geophysics. Elsevier, Amsterdam

Kopsiaftis G, Mantoglou A, Giannoulopoulos P (2009) Variable density coastal aquifer models with application to an aquifer on Thira Island. Desalination 237(1–3):65–80

Llopis-Albert C, Pulido-Velazquez D (2014) Discussion about the validity of sharp-interface models to deal with seawater intrusion in coastal aquifers. Hydrol Proc 28(10):3642–3654

McNeill JD (1994) Principles and applications of time domain electromagnetic techniques for resistivity sounding. Geonics Ltd. Technical Note TN-27, p 15

Mills T, Hoekstra P, Blohm M, Evans L (1988) Time domain electromagnetic soundings for mapping sea-water intrusion in Monterey County, California. Ground Water 26:771–782

Milnes E, Renard P (2004) The problem of salt recycling and seawater intrusion in coastal irrigated plains: an example from the Kiti aquifer (Southern Cyprus). J Hydrol 288(3–4):327–343

Nabighian MN, Macnae JC (1991) Time domain electromagnetic prospecting methods. Electromagn Methods Appl Geophys Tulsa 2:427–520

Panagopoulos G, Giannakakos E, Manoutsoglou E, Steiakakis E, Soupios P, Vafidis A (2013) Definition of inferred faults using 3-D geological modeling techniques: a case study in Tympaki basin in Crete, Greece. In: Bulletin of the Geological Society of Greece, vol. XLVII 2013 Proceedings of the 13th International Congress, Chania, Sept 2013

Panday S, Huyakorn PS, Robertson JB, Mcgurk B (1993) A density-dependent flow and transport analysis of the effects of groundwater development in a fresh-water lens of limited areal extent—the Geneva Area (Florida, USA) case-study. J Contam Hydrol 12(4):329–354

Paniconi C, Khlaifi I, Lecca G, Giacomelli A, Tarhouni J (2001) A modelling study of seawater intrusion in the Korba Coastal Plain, Tunisia. Phys Chem Earth Pt B 26(4):345–351

Papadopoulou MP, Karatzas GP, Koukadaki MA, Trichakis Y (2005) Modeling the saltwater intrusion phenomenon in coastal aquifers—a case study in the industrial zone of Herakleio in Crete Global NEST Journal 7, 2 July 2005 Issue on Water Quality, pp 197–203

Papadopoulou MP, Varouchakis EA, Karatzas GP (2010) Terrain discontinuity effects in the regional flow of a complex karstified aquifer. Environ Model Assess 15(5):319–328

Paritsis SN (2005) Simulation of seawater intrusion into the Tympaki aquifer, South Central Crete, Greece. Report within MEDIS project, Study implemented on behalf of the Department of Management of Water Resources of the Region of Crete, Heraklion, Crete, Greece

Pool M, Carrera J (2011) A correction factor to account for mixing in Ghyben-Herzberg and critical pumping rate approximations of seawater intrusion in coastal aquifers. Water Resour Res 47:W05506

Reilly TE, Goodman AS (1985) Quantitative-analysis of saltwater fresh-water relationships in groundwater systems—a historical-perspective. J Hydrol 80(1–2):125–160

Reynolds JM (2010) An introduction to applied and environmental geophysics. Wiley, New York. ISBN-13:9780471485353

Sharma P (1997) Environmental and engineering geophysics. Cambridge University press, Cambridge

Soupios P, Kalisperi D, Kanta A, Kouli M, Barsukov P, Vallianatos F (2010) Coastal aquifer assessment based on geological and geophysical survey, North Western Crete, Greece. Environ Earth Sci 61(1):63–77

Soupios P, Kourgialas N, Dokou Z, Karatzas G, Panagopoulos G, Vafidis A, Manoutsoglou E (2014) Modeling saltwater intrusion at an agricultural coastal area using geophysical methods and the FEFLOW model. IAEG XII CONGRESS, Torino, 15–19 September 2014

Stewart M, Gay MC (1986) Evaluation of transient electromagnetic soundings for deep detection of conductive fluids. Ground Water 24:351–356

Vafidis A, Soupios P, Economou N, Hamdan H, Andronikidis N, Kritikakis G, Panagopoulos G, Manoutsoglou E, Steiakakis E, Candansayar E, Schafmeister MT (2014a) Seawater intrusion imaging at Tybaki, Crete, Greece, using geophysical data and joint inversion of electrical and seismic data. First Break 32:107–114

Vafidis A, Kritikakis G, Andronikidis N, Economou N, Hamdan H, Manoutsoglou E, Steiakakis E, Candansayar E, Schafmeister MT, Kritsotakis M (2014b) Saltwater intrusion imaging at Tybaki (Greece) using geophysical methods. In: 20th European meeting of environmental and engineering geophysics, Athens, Greece, 14–18 September 2014

Xue Y, Xie CH, Wu JC, Liu PM, Wang JJ, Jiang QB (1995) A 3-dimensional miscible transport model for seawater intrusion in China. Water Resour Res 31(4):903–912